FULL PAPER

Synthesis of flow-compatible Ru-Me/Al$_2$O$_3$ catalysts and their application in hydrogenation of 1-iodo-4-nitrobenzene

Michael Sebek[1] · Hanan Atia[1] · Norbert Steinfeldt[1]

Abstract

The development of an active, selective, and long-term stable heterogeneous catalyst for the reductive hydrogenation of substituted nitroarenes in continuous operation mode is still challenging. In this work, Ru based nanoparticles catalysts promoted with different transition metals (Zn, Co, Cu, Sn, or Fe) were supported on alumina spheres using spray wet impregnation method. The freshly prepared catalysts were characterized using complementary methods including scanning transmission electron microscopy (STEM) and temperature programmed reduction (TPR). The hydrogenation of 1-iodo-4-nitrobenzene served as model reaction to assess the catalytic performance of the prepared catalysts. The addition of the promotor affected the reducibility of Ru nanoparticles as well as the performance of the catalyst in the hydrogenation reaction. The highest yield of 4-iodoaniline (89 %) was obtained in a continuous flow process using Ru-Sn/Al$_2$O$_3$. The performance of this catalyst was also followed in a long-term experiment. With increasing operation time, a catalyst deactivation occurred which could only briefly compensate by an increase of the reaction temperature.

Keywords Ruthenium · Nitro group · Reduction · Hydrogen · Flow process

Introduction

Functionalized anilines are valuable intermediates in the pharmaceutical, agrochemical, and fine chemical industries [1]. Catalytic hydrogenation of a nitroaromatic compounds to anilines using molecular hydrogen is compared to alternative processes an environmentally preferable approach [2]. Challenges arise for polyfunctional nitroarenes, due to competing reactions, i.e., hydro-dehalogenation and/or reduction of unsaturated functionalities (CC, CO, and CN) when present [3, 4]. Precious metals (Au [3, 5], Pd [6, 7], Pt [8–11], Ru [12–16]) as well as transition metals (Ni [17–19], Co [20–22], Fe [23, 24]) are used as active elements at which nitroaromatics are selectively converted into the desired amines. Compared to transition metals, precious metals generally show higher productivity in formation of the amines [25]. Their catalytic performance can be further improved if instead of the monometallic a bimetallic catalyst is used where

a transition metal is added as a promotor to an active noble metal (e.g. Pt-Zn, Ru-Cu) [16, 26].

Continuous flow operation for solid/liquid/gas multiphase reactions offers several advantages over batch operation, which explains its increasing importance for process chemists [27–33]. Small diameter packed-bed reactors offer excellent heat exchange and mass transfer due to their high surface to volume ratios and short diffusions paths. Furthermore, temperature, contact time and pressure can be precisely controlled and adjusted. Therefore, exothermic reactions can be well controlled which facilitates the safe operation even at higher temperatures and pressures [28, 34]. This allows clean transformations in cases that have previously suffered from selectivity issues, e.g. processes where the desired product can undergo follow-up reactions. Furthermore, product isolation can be simplified and process waste levels can be reduced [35]. Up on performing the reaction on a solid catalyst, it should meet the hydrodynamic requirements of the reactor to ensure uniform process conditions throughout the catalyst bed. Hence, suitable particle dimensions and morphology as well as sufficient mechanical stability of the catalyst particles are pivotal to avoid high pressure drops and channel building [36]. Nonuniform liquid flow is considered as one reason that can reduce the productivity of the continuous process

✉ Norbert Steinfeldt
  norbert.steinfeldt@catalysis.de

[1] Leibniz-Institut für Katalyse e.V. (LIKAT), Albert-Einstein-Str. 29a, 18059 Rostock, Germany

[37].The reduction of 1-iodo-4-nitrobenzene to 4-iodoaniline (scheme 1) by molecular hydrogen can be used as a model reaction for studying the reduction of nitro group in the presence of ring substituents in a continuous flow process. The iodine substituent is very prone to hydro-dehalogenation and a catalyst showing high chemoselectivity to the target product 4-iodoaniline in this reaction should be also applicable for the reduction of nitroarenes with substituents like chlorine or bromine [16]. The reductive hydrogenation of nitroarenes to anilines is a highly exothermic process, and at elevated reaction temperatures generally higher pressures are required to achieve sufficient solubility of the hydrogen gas in the organic solvent [28, 35, 38]. Recently, different Co-based catalysts were developed and tested in the continuous process applying the above model reaction. These catalysts showed high yields above 90 % with high selectivity (90 %) towards the target product 4-iodoaniline and less than 2 % yield of the undesired side product aniline [25, 36, 39]. However, both 1-iodo-4-nitrobenzene conversion as well as yield of 4-iodoaniline decreased with increasing operation time [36, 39]. The deactivation of the Co based catalyst seems to be influenced from the substrate concentration [39] and was attributed at least partly to Co leaching from the catalyst surface [36].

Although Ru is widely used as an active element in the hydrogenation reactions, its application in continuous flow process is rarely reported [35, 37, 40, 41]. Moreover, it was reported that in nitro group reduction Ru shows higher selectivity to the desired halogenated anilines than the more active Pt or Pd [38]. For that reason, flow compatible monometallic Ru/Al$_2$O$_3$ as well as bimetallic Ru-Me/Al$_2$O$_3$ catalysts were synthesized and applied for the selective reduction of 1-iodo-4-nitrobenzene to 4-iodoaniline. The aim of the presented work was (a) to elucidate the performance of the Ru/Al$_2$O$_3$ catalyst for application in a flow process in reduction of nitro group, (b) to find out whether the addition of promotors can improve the chemoselectivity of the Ru based catalyst, and (c) to evaluate their long-term stability.
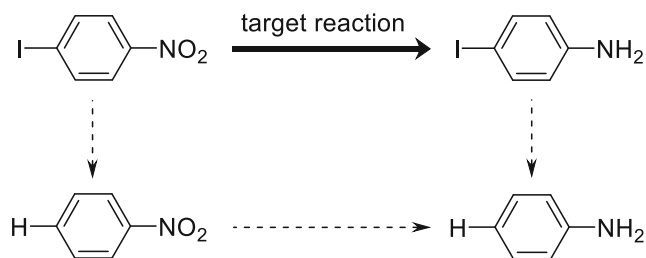
Scheme 1 Simplified reaction scheme for hydrogenation of 1-iodo-4-nitrobenzene to 4-iodoaniline using molecular hydrogen including side products formed by hydro-deiodination (for detailed reaction mechanism see e.g. ref [38])

Results and discussion

Catalyst characterization

XRD powder patterns of the different catalysts are presented in Fig. 1A. All studied samples showed only reflections of alumina phase (CCDD 00-046-1131). Reflections from Ru or the promotor were not detected indicating that the structures formed might be X-ray amorph or small and highly dispersed. SEM images from the Ru/Al$_2$O$_3$ catalyst are presented in Fig S3 to S6. The image of a single sphere of the Ru/Al$_2$O$_3$ catalyst is shown in Fig. S3. From Fig. S4 it can be seen the surface of the alumina sphere is rough and rugged. The bright dots indicate the presence of larger Ru-containing structures, but their number is only small. Fig. S5 and S6 demonstrate that the Ru is mainly located on the outer surface of the aluminum spheres and that the Ru content decreases rapidly with increasing distance from the outer surface. Moreover, Fig. S5 shows that the Ru is homogenous distributed on the outer alumina surface. To obtain further information about the size and distribution of the Ru particles deposited on the Al$_2$O$_3$ surface, the Ru/Al$_2$O$_3$ catalyst was investigated with STEM. For the first study, the catalyst beads were completely grounded into fine powder. No Ru particles could be detected because in the powder sample the proportion of the surface area on which the Ru particles are deposited is small compared to the total surface area of the powdered sample. Therefore, a small amount of material from the surface of the Ru/Al$_2$O$_3$ spheres was scraped off and again investigated with STEM. The HAADF-STEM image (Fig. 1B) of this sample showed that on applying spray wetness impregnation method mostly small Ru nanoparticles in the size range of 1–2 nm were formed and equally distributed on the outer surface of the alumina spheres.

The metal loadings of the different catalysts were determined by ICP-OES and results are summarized in Table 1. The actual Ru and promotor loadings were slightly lower than their nominal loadings (0.5 wt%) and varied between 0.32 and 0.44 wt%. The decline in the actual loading indicates that a certain part of the sprayed Ru or promotor solution was not deposited on the alumina surface during the spraying process. The BET surface area of the metal loaded catalysts varied between 154 and 197 m^2/g. TPR profiles of Ru/Al$_2$O$_3$ and the promoted Ru-Me/Al$_2$O$_3$ catalysts are presented in Fig. 2. XPS spectra of the Ru/Al$_2$O$_3$ catalyst (not shown) gave strong indication that Ru was partly oxidized during the storage of the catalyst under ambient conditions. Therefore, two reduction steps were performed. Before the first reduction was carried out, the catalyst was pretreated in an inert atmosphere at 200 °C to remove adsorbed water. The TPR profiles of the 1st reduction (Fig. 2A) showed a relatively broad reduction peak with a maximum between 83 and 90 °C. The maximum temperature of the reduction peak was slightly lower than that of

Fig. 1 **A** XRD patterns of powderd Ru-Me/Al_2O_3 samples (a) Al_2O_3 support, (b) Ru/Al_2O_3, (c) Ru-Zn/Al_2O_3, (d) Ru-Co/Al_2O_3, (e) Ru-Cu/Al_2O_3, (f) Ru-Sn/Al_2O_3, and (g) Ru-Fe/Al_2O_3 and **B** HAADF-STEM image of Ru-NP on alumina (scale bar = 20 nm)
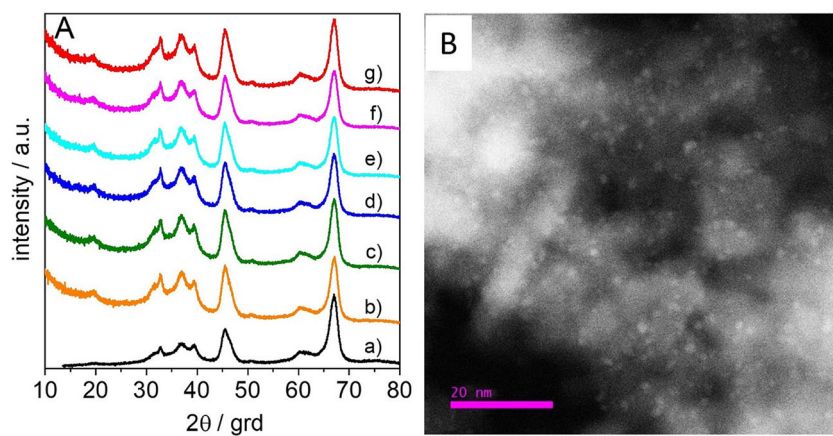
bulk RuO_2 [42] and was similar to that obtained for Ru/Al_2O_3 [43]. This broad peak is mainly attributed to the reduction of oxidized Ru species which are formed on alumina surface during catalyst storage under ambient conditions. The position of the peak maximum was shifted to slightly higher temperatures for the promoted catalyst except the catalyst promoted with Cu. All investigated catalysts also showed some hydrogen consumption at temperatures between 200 and 500 °C which was most pronounced for the Ru-Cu/Al_2O_3 catalyst. A reduction peak at 300 °C was previously reported for the reduction of Cu^{2+} [16]. The molar ratio between the Ru amount deposited on the alumina surface and the number of consumed hydrogen molecules of the first reduction cycle was approximately 1 for Ru/Al_2O_3, Ru-Zn/Al_2O_3, Ru-Co/Al_2O_3, and Ru-Cu/Al_2O_3 (see Table 1) indicating the presence of Ru^{4+} and Ru metal. However, Ru-Sn/Al_2O_3 and the Ru-Fe/Al_2O_3 catalyst displayed a ratio of 0.5 suggesting that more Ru were in the oxide form Ru^{4+}. The lower value of this ratio for the samples promoted with Fe or Sn indicates that in these samples the oxidation state of Ru during storage in air was higher than in the other samples.

The second TPR profile (Fig. 2B), obtained after oxidation of the reduced sample differed from first one. The new profiles showed either 2 maxima or a maximum together with a shoulder at temperatures below 150 °C typically for the reduction profile of RuO_2 [42]. The maximum for the Ru/Al_2O_3 catalyst occurred at the same temperature (86.1 °C) as found for the first reduction. The presence of the promotor shifted this maximum to higher temperatures in comparison to the 1st reduction. The temperature shift was increasing in the following order: Ru-Zn/Al_2O_3 < Ru-Co/Al_2O_3 < Ru-Cu/Al_2O_3 = Ru-Sn/Al_2O_3 < Ru-Fe/Al_2O_3. The amount of hydrogen consumed in the 2nd reduction was generally higher than in the 1st reduction (Table 1). Ru/Al_2O_3, Ru-Zn/Al_2O_3, and Ru-Co/Al_2O_3 revealed a comparable hydrogen consumption that corresponds approximately to the amount necessary for a complete reduction of RuO_2 to metallic Ru (2 mol hydrogen per mol Ru). Moreover, no other peaks were found for these samples in the high temperature range (300–500 °C) which means that the reduction is completed at 150 °C. The similarity between the TPR profile of Ru/Al_2O_3 and both Ru-Co/Al_2O_3 and Ru-Zn/Al_2O_3 hints that the interactions between Ru and Zn or Co

Table 1 Main characteristics of the prepared Ru-Me/Al_2O_3 catalysts

Metal						TPR			
						H$_2$-consumption		molar Ru/H$_2$ ratio	
	S_{BET} m^2/g	Ru* wt%	promotor* wt%	Ru µmol/g	promotor µmol/g	1st µmol/g	2nd µmol/g	1st -	2nd -
Ru	161	0.41	-	40.6	0	34.8	77.7	1.17	0.52
Ru-Zn	197	0.42	0.31	41.6	47.4	45.5	83.5	0.91	0.50
Ru-Co	181	0.41	0.40	40.6	67.9	40.1	82.5	1.01	0.49
Ru-Cu	189	0.34	0.44	33.6	69.2	33.1	129.6	1.01	0.26
Ru-Sn	197	0.32	0.40	31.7	33.6	64.2	126.0	0.49	0.25
Ru-Fe	154	0.35	0.42	35.1	75.2	73.4	108.0.	0.47	0.32

*obtained from ICP

Fig. 2 TPR profiles of different catalysts (**A**) first reduction step (the peak intensity was multiplied by 2.2 compared to B) and (**B**) second reduction (a) Ru/Al$_2$O$_3$, (b) Ru-Zn/Al$_2$O$_3$, (c) Ru-Co/Al$_2$O$_3$, (d) Ru-Cu/Al$_2$O$_3$, (e) Ru-Sn/Al$_2$O$_3$, and (f) Ru-Fe/Al$_2$O$_3$, (between first and second reduction step the catalyst was oxidized by heating the sample in air)
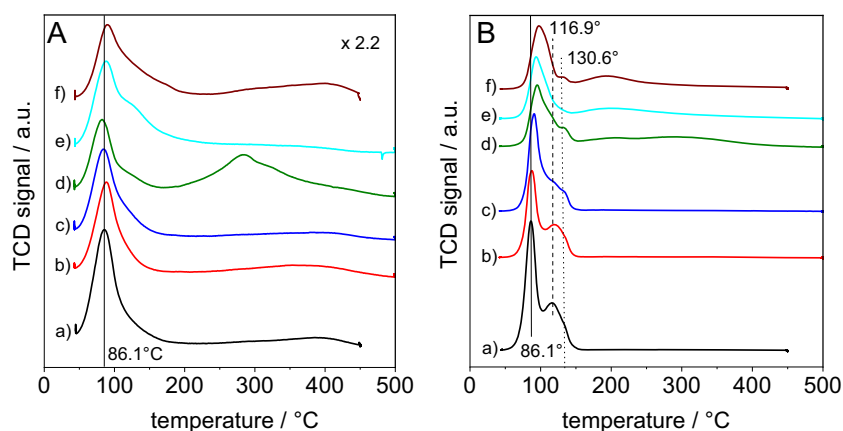
promoter only seems to be relatively small. The oxidation step following the first reduction may have led to the formation of zinc or cobalt aluminate precursors. Zinc or cobalt aluminates are probably only reduced at temperatures above 800 °C [44]. The larger shift of the peak maximum to higher temperatures in the TPR profiles of Ru-Cu/Al$_2$O$_3$, Ru-Sn/Al$_2$O$_3$ or Ru-Fe/Al$_2$O$_3$ indicates that the interaction between Ru and the promoter in these samples should be stronger compared to the other ones. Moreover, the amount of consumed hydrogen for these catalysts was significantly higher than the theoretical value necessary to reduce RuO$_2$ to metallic Ru revealing that partially Cu, Sn, or Fe oxide species [43] were also reduced by hydrogen. Reduction of bulk SnO$_2$ and of SnO$_2$ particles deposited on alumina occurred at temperatures higher than 600 °C [42, 45] and reduction of alumina supported Fe$_2$O$_3$ starts at temperatures higher than 400 °C [46].

Batch performance of Ru-Me/Al$_2$O$_3$ catalysts

The catalytic performance of the spherically Ru based catalysts was firstly tested in a small batch reactor in order to identify active and selective catalysts suitable for application in the flow process. Here, the catalysts were freshly reduced in an external tube furnace before the material was added fast to the THF/H$_2$O solvent containing the 1-iodo-4-nitrobenzene substrate. The THF/H$_2$O ratio of 95v : 5v was previously identified as the optimal solvent mixture for this reaction [25].

Table 2 presents results obtained with the different catalysts. Promotion of Ru with Zn increased the yield of 4-iodoaniline and aniline slightly to 78 and 4 %, respectively, without strongly affecting the 1-iodo-4-nitrobenzene conversion rate (Table 2, Entry 2). On the addition of cobalt both 1-iodo-4-nitrobenzene conversion rate as well as 4-iodoaniline yield decreased in comparison to the unpromoted Ru/Al$_2$O$_3$ catalyst. Moreover, aniline yield was about three times higher compared to the unpromoted catalyst. The addition of tin also reduces the catalytic activity compared to the unpromoted Ru/Al$_2$O$_3$ catalyst, but it has only a minor influence on the yield

of 4-iodoaniline (Table 2, Entry 4). In contrast, the yield of aniline increases after promotion with Sn. As Ru was promoted with Cu (Table 2, Entry 5), the yield of 4-iodoaniline increased by 3 % compared to that obtained with Ru/Al$_2$O$_3$ while aniline formation was not changed. The highest yield of 4-iodoaniline (83 %) together with the lowest yield of aniline (2 %) was obtained with the Ru-Fe/Al$_2$O$_3$ catalyst. Yield of nitrobenzene (not shown) was always very low which agreed well with previous results that show that 4-iodoaniline is more prone to dehalogenation than the starting compound 1-iodo-4-nitrobenzene [25].

It should be noted that in all experiments the carbon mass balance was incomplete. This indicates that not all products could be identified with the applied analytical method and/or some of them remained adsorbed on the catalyst surface. A reaction pathway which would reduce at least temporally the yield of aniline is the formation of azoxybenzene by condensation reaction between the nitroso and the hydroxyl amine intermediates. However, hydrogenation of this compound leads finally also to the formation of the desirable halogenated aniline [38]. GC peak area attributed to hydroxyl amine was always very low and the yield of 4-iodoaniline does not increase after 1-iodo-4-nitrobenzene was completely converted.

Table 2 Performance of Ru-Me/Al$_2$O$_3$ catalysts in the batch hydrogenation of 1-iodo-4-nitrobenzene (results are compared at time showing full substrate conversion, I-AN − 4-iodoaniline, AN - aniline)

entry	catalyst metal/Al$_2$O$_3$	time* [h]	Y(I-AN) [%]	Y(AN) [%]	C$_{balance}$ [%]
1	Ru	1.5	77	3	80
2	Ru-Zn	2.0	78	4	82
3	Ru-Co	2.0	72	10	82
4	Ru-Sn	2.5	78	6	84
5	Ru-Cu	2.5	80	3	83
6	Ru-Fe	3.5	83	2	85

*time at which conversion of 1-iodo-4-nitrobenzene reached 99.9 %

Moreover, the following decrease in the yield of 4-iodoaniline can be nearly exclusively attributed to hydrodehalogenation of 4-iodoaniline. Therefore, it is believed that beside 4-iodoaniline and aniline high molecular weight side products were formed, which are not detectable by GC [36].

As mentioned before, aniline is mainly formed by a follow-up hydrodehalogenation reaction of 4-iodoaniline in presence of the catalyst. Therefore, it can be considered as an intermediate. A continuous flow process allows a precise control of contact time which is expected to affect the product selectivity. For that background, experiments were accomplished on the Ru-Me/Al$_2$O$_3$ catalysts under continuous flow operation.

Performance of Ru-Me/Al$_2$O$_3$ in continuous flow process

Since the Ru-Co/Al$_2$O$_3$ catalyst showed poor performance in batch, it was not studied under flow conditions. The molar ratio of hydrogen to 1-iodo-4-nitrobenzene (I-NB) substrate flow was about 6 : 1 (0.15 mmol·min^{-1} H$_2$, 0.025 mmol·min^{-1} substrate). This corresponds to a twofold excess of hydrogen, since 3 mol of H$_2$ are necessary to reduce 1 mol of the nitro group to the corresponding amine. A pressure of 50 bar was chosen to dissolve a sufficient amount of hydrogen in the reaction solution. Assuming that the void in the catalyst bed is not greater than 40 % [47], the mean contact time of the liquid phase with the catalyst bed at a flow rate of 0.5 mL·min^{-1} was not longer than 1.1 min and increased to 2.2 min when the flow rate was reduced to 0.25 min. Along with the applied reaction conditions complete substrate conversion was attained at 80 °C within 1 h and remained constant over 6 h (Fig. 3). Nitrobenzene was not detected in the flow process. With the unpromoted Ru/Al$_2$O$_3$ catalyst the loss in 4-iodoaniline (I-AN) yield within 6 h was about 7 %. A minor decrease in 4-iodoaniline yield with increasing operation time was also found using the catalysts containing Zn or Cu as promotor. The highest 4-iodoaniline yield in flow operation was obtained with the Ru-Sn/Al$_2$O$_3$ and the yield increases within 6 h from 81 to 84 %. Assuming a 4-iodoaniline yield of 84 % the productivity of 4-iodoaniline in the continuous process with the Ru-Sn/Al$_2$O$_3$ catalyst amounted to 39.8 mmol·h^{-1}·mmol Ru^{-1} that is higher than that reported for Co-based catalysts [39]. The presence of the promotor had also an influence on the aniline yield. Relatively high aniline yields after 1 h (4 %) were obtained with unpromoted Ru and with the Ru-Sn/Al$_2$O$_3$ catalysts.

However, in all continuous flow hydrogenations the catalysts showed with ongoing operation time a steady decrease of the aniline yield to lower than 2 % after 2 h of reaction. After 7 h operation time, the continuous flow experiment was interrupted, the reactor was cooled down and the catalyst was stored inside the reactor under pure THF at 25 °C for about 16 h. Next day, the reaction was continued under the
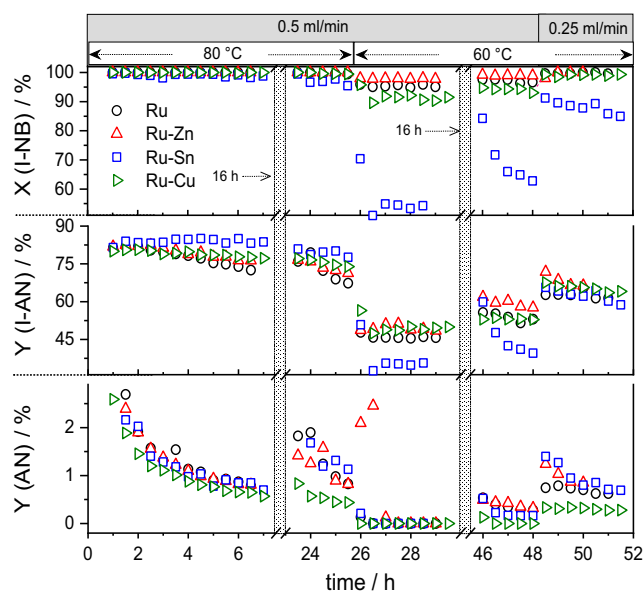

Fig. 3 Plot of 1-iodo-4-nitrobenzene (I-NB) conversion, and yields of 4-iodoaniline (I-AN) and aniline (AN) versus time for Ru-Me/Al$_2$O$_3$ catalysts in continuous flow process (1 g Ru-Me/Al$_2$O$_3$ catalyst, 80 °C, 50 bar, F$_{gas}$ = 3.6 mL·min^{-1}, 0.05 M 1-iodo-4-nitrobenzene in THF/H$_2$O (95v/5v), 16 h: the catalyst was stored in the reactor for 16 h in THF at room temperature)

same conditions as previously reported. On the second day the conversions of 1-iodo-4-nitrobenzene were comparable to the 1st day. However, on increasing operation time, a drop in 1-iodo-4-nitrobenzene conversion as well as 4-iodoaniline yield was observed for all catalysts. Aniline formation showed on the second day the same trend as observed on the first day experiments, but the yields were slightly higher.

After 3 h operation at 80 °C, the reaction temperature was reduced to 60 °C. At this temperature, significant differences in the catalytic performance between the four catalysts were observed. Conversion of 1-iodo-4-nitrobenzene at 60 °C was in the range 54–98 % and decreased in the following order: Ru-Zn ≈ Ru > Ru-Cu >> Ru-Sn. With the reduce of temperature from 80 to 60 °C yield of 4-iodoaniline diminished too and achieved for Ru, Ru-Zn, and Ru-Cu values between 45 and 48 %. The Ru-Sn catalyst showed the lowest 4-iodoaniline yield (35 %). Aniline was detected only in traces at this condition. Within the next four hours (26–30 h), all catalysts displayed a stable performance. Subsequently, the reaction was again interrupted, and the catalyst was stored in the reactor at room temperature under THF for the next 16 h. After then, the reaction started using identical reaction parameters as the day before. For Ru, Ru-Zn, and Ru-Cu catalysts substrate conversion and 4-iodoaniline yield were slightly higher as obtained at the day before. In contrast, the performance of the Ru-Sn catalyst was not stable and both 1-iodo-4-nitrobenzene conversion as well as 4-iodoaniline yield diminish with increasing operation time. After a total time of 48 h, the flow rate was reduced from 0.5 to 0.25 mL·min^{-1}. For Ru,

Ru-Zn, and Ru-Cu, the 1-iodo-4-nitrobenzene conversion rose to 100 %, and the yield of 4-iodoaniline increased from 53 to about 65 %. The lowest yield of aniline under these conditions was obtained with the Ru-Cu catalyst (< 0.4 %). As already observed for the shorter contact time, the 1-iodo-4-nitrobenzene conversion of the Ru-Sn catalyst decreased with increasing time, but the yield of 4-iodoaniline was like to the other three catalysts.

The catalytic behavior of the Ru-Fe catalyst using the same reaction initial parameters as applied for the other catalysts is presented in Fig. 4. As already observed for the other four catalysts 1-iodo-4-nitrobenzene conversion was stable at 100 % within the first 7 h. Yield of 4-iodoaniline reached its maximum (82 %) after 1.5 h and decreased only slightly with increasing operation time. The yield of aniline was below 0.5 %, which was the lowest for all catalysts studied. After interruption of the reaction and storage the catalyst under THF the hydrogenation was continued using the same parameters as before on the second day 1-iodo-4-nitrobenzene conversion and 4-iodoaniline yield slightly decreased with increasing operation time. After 12 h of operation, the decrease in 1-iodo-4-nitrobenzene conversion and in 4-iodoaniline yield was 2 and 10 %, respectively. The aniline yield was again very low.

The highest initial yield of 4-iodoaniline was obtained in the flow process with those promoters (Fe and Sn) exhibiting in the TPR experiment the strongest interaction with Ru. Previously, it was suggested that coordinatively unsaturated Sn^{4+} or Sn^{2+} species formed in reducing atmosphere may activate the polar NO_2 groups [15]. Otherwise, the similar behavior of the Ru and the Ru-Zn catalyst might be explained with the low interaction between Ru and Zn.
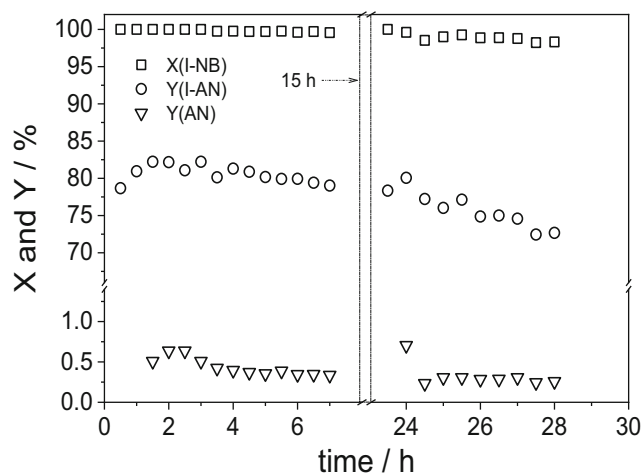
This assumption was supported by ICP results of spent catalysts. Lower Ru content (between 2 and 6 %) in all spent catalysts was found indicating leaching of Ru from the catalyst surface into the reaction solution was only low. On the other hand, catalysts promoted with a second metal, the number of species leached depends on the type of metal. The catalysts Ru-Zn, Ru-Cu, Ru-Sn showed a Zn, Cu and Sn loss of 48 %, 11 %, and 1 %, respectively. The high Zn loss might be explained with the low interaction between Ru and Zn as it has been demonstrated previously by TPR results. In contrast, Sn containing sample showed lower Sn leaching due to strong interaction between Ru and Sn. Additionally, the amount of iodine on the spent catalyst was also determined. The presence of iodine might result from adsorbed iodine containing compounds or from metal iodides formed during the reaction. The iodine content of Ru, Ru-Zn, Ru-Cu, and Ru-Fe catalysts was found to be between 1.1 and 1.4 wt%, while more iodine content of 3.9 wt% on Ru-Sn catalyst was attained. The high iodine content of the Ru-Sn catalyst might be attributed to a reaction between the promotor Sn and iodine which seems to occur with the other used promoter metals in clearly lower extent.

Ru-Sn/Al_2O_3 exhibited the highest initial 4-iodoaniline yield in the flow process but its performance in the long-term experiment differs from that of the other catalysts. To exclude that interruption of reaction has an influence on the observed low catalytic stability, a new long-term experiment was performed with this catalyst without any interruption. In comparison to the previous flow experiments the 1-iodo-4-nitrobenzene concentration was doubled (0.1 M) and the reaction temperature was increased from 80 to 100 °C. Since both, the bed volume and liquid phase flow rate were reduced by half, the contact time and hydrogen to substrate ratio remained nearly constant. The results of this experiment are presented in Fig. 5. As shown, within the first 7 h high conversion rates between 98 and 100 % of 1-iodo-4-nitrobenzene with a maximum 4-iodoaniline yield of 89 % (4 h) were observed. In the ongoing flow process the catalyst activity decreased continuously to a minimum conversion of 82 % of the starting compound resulting in a low yield of 65 % 4-iodoaniline. The temporal evolution of aniline formation was different from that of 4-iodoaniline. The yield of aniline dropped strongly within the first 4 h of reaction from 8 % (1 h) to around 2 %. With longer operation time the decrease in aniline yield over the following 16 h was relatively low compared to that which was observed in the first hours of the flow process. The results show that the Ru-Sn/Al_2O_3 catalyst was strongly deactivated already within a period of 16 h. Next, it was investigated whether an increase of the contact time could compensate the deactivation. A reduction of the flow rate to 0.2 mL/min in the process gave only a slightly
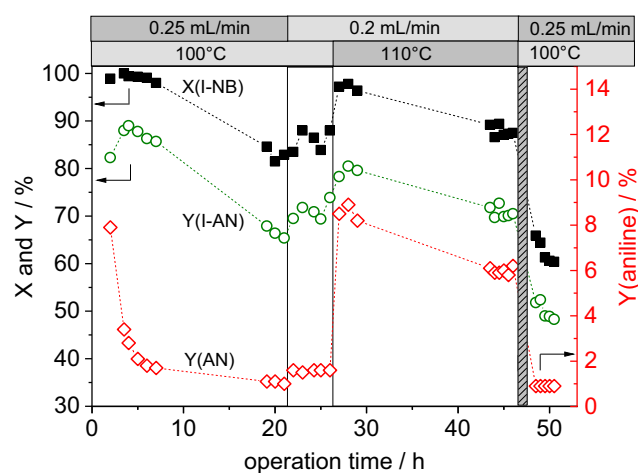

Fig. 4 Plot of 1-iodo-4-nitrobenzene (I-NB) conversion, and yields of 4-iodoaniline (I-AN) and aniline (AN) versus time for Ru-Fe/Al_2O_3 catalyst in continuous flow process (1 g Ru-Me/Al_2O_3 catalyst, 80 °C, 50 bar, F_{gas} = 3.6 mL·min^{-1}, F_L = 0.5 mL·min^{-1}, 0.05 M 1-iodo-4-nitrobenzene in THF/H_2O (95v/5v), 15 h: the catalyst was stored in the reactor for 15 h in THF at room temperature)

Fig. 5 Plot of 1-iodo-4-nitrobenzene conversion (I-NB) and yield of 4-iodoaniline (I-AN) and aniline (AN) versus operation time using Ru-Sn/Al$_2$O$_3$ catalysts in continuous flow process, variable parameters: liquid phase flow rate (column 1) and reaction temperature (column 2); constant parameters: 0.58 g Ru-Sn/Al$_2$O$_3$ catalyst, 50 bar, F_{H2} = 3.6 mL/min, 0.1 M 1-iodo-4-nitrobenzene in THF/H$_2$O (95v/5v)

higher substrate conversion and 4-iodoaniline yield (see results between 22 and 26 h).

An increase of the reaction temperature from 100 to 110 °C leads to a significant higher conversion of the 1-iodo-4-nitrobenzene as well as higher 4-iodoaniline yield. When performing the hydrogenation at 110 °C, the 1-iodo-4-nitrobenzene conversion raised briefly to 95 % and the yield of 4-iodoaniline increased to about 80 %. However, with increased time of process, both values dropped again continuously but in a less extent as observed within the first 16 h. Otherwise, due to the increase of the temperature to 110 °C it was around 4 times more aniline produced compared to that reaction at 100 °C. Nitrobenzene was not detected in the continuous flow operation. The strong increase of the aniline yield shows that the hydro-dehalogenation reaction is more affected by temperature as the nitro group reduction. This observation was already reported for Co based catalyst [38, 39]. Products formed by hydrogenation of the aromatic ring, observed previously at hydrogenation of nitrobenzene using a Ru/CNT catalyst [42], were also not detected. After a period of 46 h the process parameters were adjusted to that applied at the beginning of the experiment (100 °C, 0.25 mL/min). The conversion of 1-iodo-4-nitrobenzene and the yield of 4-iodoaniline at that point were approximately 40 % lower compared with the fresh catalyst.

Within the whole experiment a steady state with a constant catalytic performance was not observed. A plot exhibiting product selectivity versus operation time (see Fig. S7) shows that 4-iodoaniline selectivity was

relatively stable between 80 and 90 % over the whole experiment including that time were aniline yield increased by 400 %. Deactivation of the catalyst could be caused by Ru metal leaching from catalyst surface into the solution or by blocking the catalytically active surface sites responsible for the reduction of the nitro group. To find out whether Ru was leached from the catalyst, the collected reaction mixture was treated in a rotary evaporator. The residue from this process was heated in Ar flow at 500 °C (3 h) to reduce its mass. After heating, the Ru weight found in the black residual was 0.002 wt% which corresponds to a Ru leaching of 0.7 %. This is in agreement with the ICP results of the spent catalyst which showed a Ru and Sn loss of 3.7 and 10.8 %, respectively. Because of these relatively low leaching values of active metal, it seems to be not the main reason for the observed catalyst deactivation. Nerveless, it might be due to the strong adsorption of high molecular weight side products and/or the halogenation of active Sn surface sites with iodine. The iodine content of the spent catalyst was found to be 2 wt%. An insufficient robustness of the alumina spheres can be excluded as reason for the observed deactivation.

In summary, Ru-Me/Al$_2$O$_3$ catalysts composed of small Ru nanoparticles deposited on the external surface of preformed alumina spheres are suitable for application in continuous flow operation using small packed-bed reactor. The addition of a metal promoter to the Ru nanoparticles affects both the reducibility of the formed Ru nanoparticles as well as the performance of the catalyst in the hydrogenation reaction depending on the added promotor.

The catalysts tested in batch operation under the same conditions the highest yield of target product 4-iodoaniline (83 %) was achieved with Fe as promotor. The Ru-Fe/Al$_2$O$_3$ catalyst also showed the lowest yield of the undesired side product aniline (2 %). The TPR results hint that interaction between Ru and the added promotor was the strongest for this catalyst.

Comparing the Ru-Me/Al$_2$O$_3$ catalysts in the flow process the highest initial yield of the target product 4-iodoaniline was obtained with the Ru-Sn/Al$_2$O$_3$ catalyst (84 %). Yield of aniline was relatively low (< 2 %). With this catalyst 4-iodoaniline yield can be further increased to 89 % if the reaction conditions were optimized. However, the Ru based catalyst showed a deactivation with time leading to a steady decrease in 1-iodo-4-nitrobenzene conversion as well as 4-iodoaniline yield. The decrease of both can be compensated only short by increasing the reaction temperature. Deactivation of this catalyst might be caused by reaction between iodine and the Sn promotor leading to formation of SnI$_2$. Ongoing research deals with process optimization and the developing of a more stable Ru-Sn/Al$_2$O$_3$ and Ru-Fe/Al$_2$O$_3$ catalysts.

Experimental section

Materials and material synthesis

Materials

1-iodo-4-nitrobenzene (98 %), diethylene glycol dibutyl ether (> 99 %), nitrobenzene (> 99 %), and aniline (99.5 %) were purchased from Sigma-Aldrich. 4-iodoaniline (> 99 %) was supplied by TCI. Tetrahydrofuran (THF, 99 %+, stabilized with butylated hydroxytoluene) was obtained from Acros Organics. Hydrogen was supplied by Air Liquide with a purity of 99.999 %. Alumina spheres 1.0/160 (Product code: 610,110, V_p: 0.45 cm^3/g) were obtained from Sasol Germany. $RuCl_3 \cdot xH_2O$ (39wt% Ru, Alfa Aesar), $Zn(NO_3)_2 \cdot 6H_2O$ (99 %, Sigma-Aldrich), $Co(NO_3)_2 \cdot 6H_2O$ (98,8 % Sigma-Aldrich), $Cu(NO_3)_2 \cdot 3H_2O$ (98 %, Sigma-Aldrich), $SnCl_2 \cdot 2H_2O$ (98 %, Sigma-Aldrich), $Fe(NO_3)_3 \cdot 9H_2O$ (99 %, Merck) were used as received.

Preparation of Ru/Al$_2$O$_3$ catalyst

The catalyst was prepared via incipient wetness impregnation by using a self-constructed spray device (see Fig. S1 and S2, Supplementary Information). First, the commercially available alumina spheres were cleaned several times with pure ethanol (EtOH), dried at 140 °C in air and stored in the vacuum desiccator. 8.50 mL of a fresh prepared aqueous solution of $RuCl_3 \cdot xH_2O$ (243.6 mg = 94.8 mg Ru) was sprayed with a rate of 0.5 mL min^{-1} on 18.9 g alumina spheres rotating in a 500 mL round bottom flask. The nominal Ru loading was 0.5 wt%. The uniformly impregnated alumina spheres were dried in air for 18 h at 60 °C and then heated under a flow of 5 % H_2/Ar (100 mL·min^{-1}) using the following heating-program: 25–120 °C/15 min, 120 °C/2 h; 120–500 °C/3 h, 500 °C/6 h. The prepared solid catalyst was left to cool down to room temperature under H_2/Argon flow. Fig. S2 shows a picture of the prepared catalyst.

Preparation of bimetallic Ru-Me/Al$_2$O$_3$ catalysts

For addition of the second metal precursor the freshly synthesized Ru/Al$_2$O$_3$ catalyst was loaded in a rotating 250 mL round bottom flask. Afterwards, a certain amount of the fresh prepared aqueous metal salt solution (see Table 3) was sprayed on the Ru/Al$_2$O$_3$ catalyst spheres to obtain a nominal molar Ru to promotor ratio of 1:1. The thermal treatment of the material after deposition of the second metal was the same as applied for preparing the monometallic Ru/Al$_2$O$_3$ catalyst.

Characterization

X-ray diffraction (XRD) powder patterns were recorded on a Panalytical X'Pert diffractometer equipped with a Xcelerator detector using automatic divergence slits and Cu Kα1 radiation (40 kV, 40 mA; $\lambda = 0.15406$ nm). For this purpose, the spheres were crushed into a fine powder before measurement. The obtained intensities were converted from automatic to fixed divergence slits (0.25°) for further analysis. Phase identification was done using the PDF-2 database of the International Center of Diffraction Data (ICDD).

Scanning transmission electron microscopy (STEM) measurements were performed at 200 kV with a probe aberration-corrected JEM-ARM200F (microscope: JEOL, Japan; corrector: CEOS, Germany) using a high angle annular dark field (HAADF) detector. The powdered sample was deposed on a holey carbon supported Cu-grid (mesh 300) without any pretreatment and transferred to the microscope.

Scanning electron microscopy (SEM) analysis was performed by a field emission scanning electron microscope (FE-SEM, MERLIN® VP Compact, Co. Zeiss, Oberkochen) equipped with an energy dispersive X-ray (EDX) detector (XFlash 6/30, Co. Bruker, Berlin). Representative areas of the samples were analyzed by QUANTAX ESPRIT Microanalysis software (version 2.0).

The Ru loading and the amount of the promotor (Zn, Co, Cu, Sn, and Fe) was determined by inductive coupled plasma-optical emission spectrometry (ICP-OES). The catalysts were chemically digested in aqua regia using a microwave (Multiwave PRO, Anton Paar). The obtained solution was measured in a Varian 715-ES ICP emission spectrometer.

An ASAP 2010 (Micromeritics) porosimeter was used to determine specific surface area (SSA) and pore volume of the spherical catalysts. The isotherms were recorded using liquid nitrogen as adsorbate at a temperature of -196 °C. The Brunauer-Emmett-Teller (BET) method was used to calculate the specific surface areas. The pore size distribution was obtained from the desorption branch of the sorption isotherm using Barrett-Joyner-Halenda (BJH) method.

H_2-Temperature Programmed Reduction (TPR) experiments were done using a Micromeritics Autochem II 2920 instrument. About 300 mg sample was loaded in U shaped quartz reactor and heated from RT to 200 °C with 20 K/min in Ar for 30 min, then cooled down to RT under Ar flow (50 mL·min^{-1}). TPR1 run (1st step) was carried out from RT to 500 °C in a 5 % H_2/Ar flow (20 mL·min^{-1}) with a heating rate of 10 K/min. Before running TPR2 (2nd step) the sample was heated from RT to 400 °C (60 min hold time) under the flow of 5 % O_2/He (50 mL·min^{-1}). The sample was cooled down and TPR2 was done. The sample was heated from RT to 500 °C in a 5 % H_2/Ar flow (20 mL·min^{-1}) with a heating rate of 10 K/min. The hydrogen consumption peaks were recorded

Table 3 Metal precursors and the solution volumes used for the synthesis of bimetallic catalysts

0.5 wt% Ru/Al$_2$O$_3$	metal precursor		solution	volume	name
g			mg/mL	mL	
3.0	Zn(NO$_3$)$_2$ · 6 H$_2$O		109.6	1.4	Ru-Zn/Al$_2$O$_3$
2.0	Co(NO$_3$)$_2$ · 6 H$_2$O		55.9	0.9	Ru-Co/Al$_2$O$_3$
2.5	Cu(NO$_3$)$_2$ · 3 H$_2$O		42.4	1.1	Ru-Cu/Al$_2$O$_3$
2.5	SnCl$_2$ · 2 H$_2$O		21.2[*]	1.1	Ru-Sn/Al$_2$O$_3$
3.0	Fe(NO$_3$)$_3$ · 9 H$_2$O		11.2	1.4	Ru-Fe/Al$_2$O$_3$

*in 0.1 M HCl

with temperature using a TCD detector. The amount of hydrogen consumed was calculated based on the peak areas.

Batch experiments

The performance of the catalysts was first evaluated in batch experiments by using a stainless-steel reactor (Parr Instruments, 0.045 L) equipped with a glass insert, magnetic stirrer (0.5 × 0.3 cm) and a sample-taking valve with dip tube. The reactor was filled with 10 mL of a THF/H$_2$O (95v/5v) solution containing 1-iodo-4-nitrobenzene (2.0 mmol; 0.508 g, 0.2 M) and diethylene glycol dibutyl ether (0.222 g; 1.0 mmol; internal standard). The catalyst mass was 100 mg (nominal Ru metal/substrate ratio = 0.25 mol%). Before heating to 110 °C, the reactor was purged four times with H$_2$ (5 bar) and pressurized with H$_2$ to 20 bar. The reaction progress was followed by sampling the reaction mixture every 0.5 h. The taken samples were diluted with THF (1:2) and analyzed by Agilent 6890 N gas chromatograph equipped

with flame ionization detector (FID) and DB-5 capillary column (length: 30 m, ID: 0.25 mm, film 0.25 μm).

Continuous flow experiments

Hydrogenation of 1-iodo-4-nitrobenzene in the continuous flow operation was performed by using a modular Ehrfeld microreaction system equipped with a cartridge reactor 240 (length = 63 mm, internal ∅ = 10 mm, V = 5 mL). The experimental set-up is shown in Fig. 6. The catalyst freshly activated in an external tube furnace (2 h, 350 °C in H$_2$/Ar – 5 vol%/ 95 vol%) was loaded inside the cartridge (1.00 g, V_{bed}= 1.34 mL, bed length = 1.70 cm) together with glass wool (0.45 g) and glass beads (3.4 g, d = 0.75 mm). The 1-iodo-4-nitrobenzene containing THF/H$_2$O solution (95v/5v) was pumped by a Knauer K-501 HPLC pump. Hydrogen flow was regulated with a mass flow controller (Bronkhorst). The hydrogen gas flow rate was 3.6 mL/min. Gas and liquid phase were mixed in a slit-plate micro mixer (model LH2) before

Fig. 6 Flowsheet for the set-up used to study the continuous process of reductive hydrogenation of 1-iodo-4-nitrobenzene with molecular hydrogen over Ru-Me/ Al$_2$O$_3$ catalysts
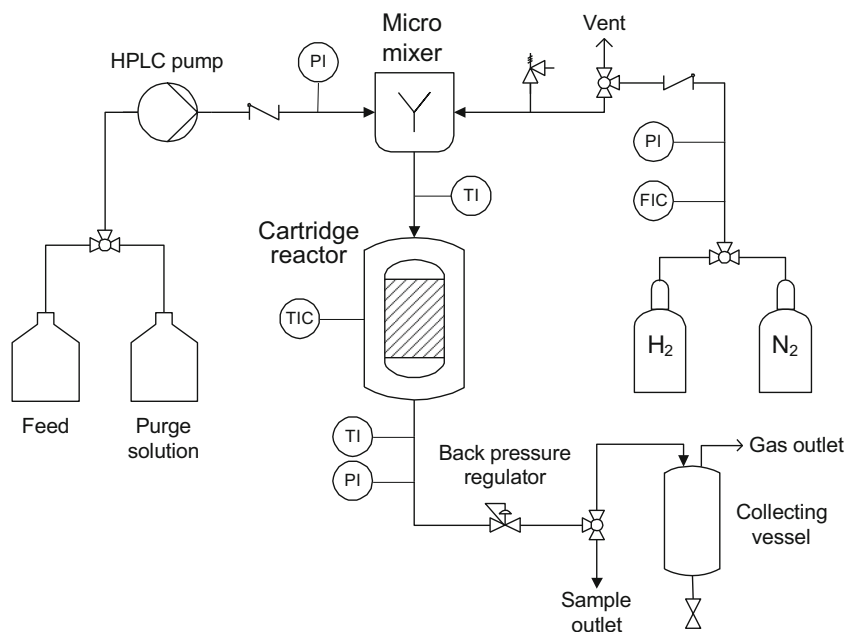
feeding the reaction mixture into the cartridge reactor. The temperature of the reaction mixture was measured inside the cartridge reactor directly before the gas liquid mixture enters the cartridge. The pressure was monitored by pressure sensor which was placed in front of the slit-plate mixer. The system pressure was adjusted by using a backpressure valve (Equilibar EB1). At the beginning of the flow experiment, the microreaction system was rinsed with 1 mL·min^{-1} THF at room temperature. The system was adjusted to the corresponding reaction parameters (T, P, flow rates of H$_2$ and liquid phase) using THF as solvent within 0.5 h. Then, THF was replaced by a THF/H$_2$O (95v/5v) solvent containing the substrate 1-iodo-4-nitrobenzene (0.05 M) and diethylene glycol dibutyl ether (0.025 M, internal standard). Samples were taken every 0.5 h and diluted with THF (1:5) for GC analysis as mentioned before.

The conversion (X) of 1-iodo-4-nitrobenzene (I-NB) and the yield of the target product 4-iodoaniline (I-AN) as well as of the side products aniline (AN) and nitrobenzene (NB) were calculated as

$$arrayX_{I-NB}[\%] = \left(c_{(I-NB)in} - c_{(I-NB)out}\right)/c_{(I-NB)in} \times 100$$

$$Y_i[\%] = -c_{(i)out}/c_{(I-NB)in} \times 100$$

$$i = I - AN, AN, NB$$

in which $c_{(I-NB)in}$ and $c_{(I-NB)out}$ are the inlet and outlet concentration of the substrate 1-iodo-4-nitrobenzene and $c_{(i)out}$ is the outlet concentration of product i in flow operation. For batch operation $c_{(I-NB)out}$ and $c_{(i)out}$ have to be replaced in the above formula by $c_{(I-NB)t}$ and $c_{(i)t}$ (t: operation time).

The long-term experiment was performed using 0.58 g Ru-Sn/Al$_2$O$_3$ catalyst. The catalyst (bed volume = 0.63 mL) was placed between two layers of glass wool directly on the bottom of the cartridge. Above the catalyst was a bed of glass spheres (diameter: 0.75–1 mm) which was also covered with a layer of glass wool. A THF/H$_2$O (95v/5v) solvent containing the substrate 1-iodo-4-nitrobenzene (0.1 M) and diethylene glycol dibutyl ether (0.05 M, internal standard) was continuously pumped through the catalyst bed. The liquid phase flow rate was adjusted to 0.20 or 0.25 mL·min^{-1}. Total pressure (50 bar) and hydrogen gas flow rate (3.6 mL·min^{-1}) were constant and not changed during the experiment. The start-up procedure was the same as described for the investigation of the different Ru-Me/Al$_2$O$_3$ catalysts. The solution leaving the reactor was collected in a 1 L stainless-steel container. Small samples were taken at different times intervals and analyzed by GC as described before.

Supplementary Information The online version contains supplementary material available at https://doi.org/10.1007/s41981-021-00159-0.

References

1. Orlandi M, Brenna D, Harms R, Jost S, Benaglia M (2018) Recent developments in the reduction of aromatic and aliphatic nitro compounds to amines. Org Process Res Dev 22:430–445. https://doi.org/10.1021/acs.oprd.6b00205

2. Blaser H-U, Steiner H, Studer M (2009) Selective catalytic hydrogenation of functionalized nitroarenes: an update. ChemCatChem 1(2):210–221. https://doi.org/10.1002/cctc.200900129

3. Serna P, Corma A (2015) Transforming nano metal nonselective particulates into chemoselective catalysts for hydrogenation of substituted nitrobenzenes. ACS Catal 5(12):7114–7121

4. Serna P, Boronat M, Corma A (2011) Tuning the behavior of Au and Pt catalysts for the chemoselective hydrogenation of nitroaromatic compounds. Top Catal 54(5–7):439–446

5. Boronat M, Concepción P, Corma A, González S, Illas F, Serna P (2007) A molecular mechanism for the chemoselective hydrogenation of substituted nitroaromatics with nanoparticles of gold on TiO$_2$ catalysts: a cooperative effect between gold and the support. J Am Chem Soc 129(51):16230–16237

6. Huang H, Wang X, Tan M, Chen C, Zou X, Ding W, Lu X (2016) Solvent-free selective hydrogenation of nitroarenes using nanoclusters of palladium supported on nitrogen-doped. Ordered Mesoporous Carbon ChemCatChem 8(8):1485–1489

7. Lyu J, Wang J, Lu C, Ma L, Zhang Q, He X, Li X (2014) Size-dependent halogenated nitrobenzene hydrogenation selectivity of Pd nanoparticles. J Phys Chem C 118(5):2594–2601

8. Du W, Xia S, Nie R, Hou Z (2014) Magnetic Pt catalyst for selective hydrogenation of halonitrobenzenes. Ind Chem Eng Res 53(12):4589–4594

9. Lara P, Philippot K (2014) The hydrogenation of nitroarenes mediated by platinum nanoparticles: an overview. Catal Sci Technol 4(8):2445–2465

10. Lara P, Suarez A, Colliere V, Philippot K, Chaudret B (2014) Platinum N-heterocyclic carbene nanoparticles as new and effective catalysts for the selective hydrogenation of nitroaromatics. ChemCatChem 6(1):87–90

11. Motoyama Y, Lee Y, Tsuji K, Yoon SH, Mochida I, Nagashima H (2011) Platinum nanoparticles supported on nitrogen-doped carbon nanofibers as efficient poisoning catalysts for the hydrogenation of nitroarenes. ChemCatChem 3(10):1578–1581

12. Oubenali M, Vanucci G, Machado B, Kacimi M, Ziyad M, Faria J, Raspolli-Galetti A, Serp P (2011) Hydrogenation of p-chloronitrobenzene over nanostructured-carbon-supported ruthenium catalysts. ChemSusChem 4(7):950–956. https://doi.org/10.1002/cssc.201000335

13. Chary KV, Srikanth CS (2009) Selective hydrogenation of nitrobenzene to aniline over Ru/SBA-15 catalysts. Catal Lett 128(1–2):164–170

14. Fan G, Huang W, Wang C (2013) In situ synthesis of Ru/RGO nanocomposites as a highly efficient catalyst for selective hydrogenation of halonitroaromatics. Nanoscale 5(15):6819–6825

15. Zuo B, Wang Y, Wang Q, Zhang J, Wu N, Peng L, Gui L, Wang X, Wang R, Yu D (2004) An efficient ruthenium catalyst for selective hydrogenation of ortho-chloronitrobenzene prepared via assembling ruthenium and tin oxide nanoparticles. J Catal 222(2):493–498

16. Pietrowski M, Zieliński M, Wojciechowska M (2011) High-selectivity hydrogenation of chloronitrobenzene to chloroaniline over magnesium fluoride-supported bimetallic ruthenium-copper catalysts. ChemCatChem 3(5):835–838

17. Hahn G, Ewert JK, Denner C, Tilgner D, Kempe R (2016) A reusable mesoporous nickel nanocomposite catalyst for the selective hydrogenation of nitroarenes in the presence of sensitive functional groups. ChemCatChem 8(15):2461–2465

18. Jiang C, Shang Z, Liang X (2015) Chemoselective transfer hydrogenation of nitroarenes catalyzed by highly dispersed, supported nickel nanoparticles. ACS Catal 5(8):4814–4818

19. Wang J, Yuan Z, Nie R, Hou Z, Zheng X (2010) Hydrogenation of nitrobenzene to aniline over silica gel supported nickel catalysts. Ind Chem Eng Res 49(10):4664–4669

20. Schwob T, Kempe R (2016) A reusable Co catalyst for the selective hydrogenation of functionalized nitroarenes and the direct synthesis of imines and benzimidazoles from nitroarenes and aldehydes. Angew Chem Int Ed 55(48):15175–15179. https://doi.org/10.1002/anie.201608321

21. Wang X, Li Y (2016) Chemoselective hydrogenation of functionalized nitroarenes using MOF-derived co-based catalysts. J Mol Catal A 420:56–65

22. Westerhaus FA, Jagadeesh RV, Wienhöfer G, Pohl M-M, Radnik J, Surkus A-E, Rabeah J, Junge K, Junge H, Nielsen M (2013) Heterogenized cobalt oxide catalysts for nitroarene reduction by pyrolysis of molecularly defined complexes. Nat Chem 5(6):537–543

23. Li Y, Zhou Y-X, Ma X, Jiang H-L (2016) A metal–organic framework-templated synthesis of γ-Fe$_2$O$_3$ nanoparticles encapsulated in porous carbon for efficient and chemoselective hydrogenation of nitro compounds. Chem Comm 52(22):4199–4202

24. Jagadeesh RV, Surkus A-E, Junge H, Pohl M-M, Radnik J, Rabeah J, Huan H, Schünemann V, Brückner A, Beller M (2013) Nanoscale Fe2O3-based catalysts for selective hydrogenation of nitroarenes to anilines. Science 342(6162):1073–1076

25. Loos P, Alex H, Hassfeld J, Lovis K, Platzek J, Steinfeldt N, Hübner S (2016) Selective hydrogenation of halogenated nitroaromatics to Haloanilines in batch and flow. Org Process Res Dev 20(2):452–464. https://doi.org/10.1021/acs.oprd.5b00170

26. Iihama S, Furukawa S, Komatsu T (2016) Efficient catalytic system for chemoselective hydrogenation of halonitrobenzene to haloaniline using PtZn intermetallic compound. ACS Catal 6(2):742–746

27. Glasnov T (2016) Continuous-flow chemistry in the research laboratory. https://doi.org/10.1007/978-3-319-32196-7

28. Cantillo D, Damm M, Dallinger D, Bauser M, Berger M, Kappe CO (2014) Sequential nitration/hydrogenation protocol for the synthesis of triaminophloroglucinol: safe generation and use of an explosive intermediate under continuous-flow conditions. Org Process Res Dev 18(11):1360–1366

29. Baumann M, Baxendale IR, Hornung CH, Ley SV, Rojo MV, Roper KA (2014) Synthesis of riboflavines, quinoxalinones and benzodiazepines through chemoselective flow based hydrogenations. Molecules 19(7):9736–9759

30. Malet-Sanz L, Susanne F (2012) Continuous flow synthesis. A pharma perspective. J Med Chem 55(9):4062–4098

31. Chen J, Przyuski K, Roemmele R, Bakale RP (2013) Improved continuous flow processing: benzimidazole ring formation via catalytic hydrogenation of an aromatic nitro compound. Org Process Res Dev 18(11):1427–1433

32. Wegner J, Ceylan S, Kirschning A (2012) Flow chemistry–a key enabling technology for (multistep) organic synthesis. Adv Synth Catal 354(1):17–57

33. Qian Z, Baxendale IR, Ley SV (2010) A flow process using microreactors for the preparation of a quinolone derivative as a potent 5HT1B Antagonist. Synlett 2010 (04):505–508

34. Cantillo D, Baghbanzadeh M, Kappe CO (2012) In situ generated iron oxide nanocrystals as efficient and selective catalysts for the reduction of nitroarenes using a continuous flow method. Angew Chem Int Ed 51(40):10190–10193

35. Irfan M, Glasnov TN, Kappe CO (2011) Heterogeneous catalytic hydrogenation reactions in continuous-flow reactors. ChemSusChem 4(3):300–316

36. Baramov T, Loos P, Hassfeld J, Alex H, Beller M, Stemmler T, Meier G, Gottfried M, Roggan S (2016) Encapsulated cobalt oxide on carbon nanotube support as catalyst for selective continuous hydrogenation of the showcase substrate 1-Iodo-4-nitrobenzene. Adv Synth Catal 358(18):2903–2911

37. Aho A, Roggan S, Eränen K, Salmi T, Murzin DY (2015) Continuous hydrogenation of glucose with ruthenium on carbon nanotube catalysts. Catal Sci Technol 5(2):953–959

38. Pietrowski M (2012) Recent developments in heterogeneous selective hydrogenation of halogenated nitroaromatic compounds to halogenated anilines. Curr Org Synth 9(4):470–487

39. Alex H, Loos P, Baramov T, Barry J, Godiawala T, Hassfeld J, Steinfeldt N (2017) Polymer encapsulated cobalt-based catalysts (Co EnCatTM) for selective continuous hydrogenation of 1-Iodo-4-nitrobenzene. ChemCatChem 9(16):3210–3217. https://doi.org/10.1002/cctc.201700391

40. Konrath R, Heutz FJ, Steinfeldt N, Rockstroh N, Kamer PC (2019) Facile synthesis of supported Ru–Triphos catalysts for continuous flow application in selective nitrile reduction. Chem Sci 10(35):8195–8201

41. Paun C, Lewin E, Sá J (2017) Continuous-flow hydrogenation of D-xylose with bimetallic ruthenium catalysts on micrometric alumina. Synthesis and Catalysis: Open Access 2(1:2):1–6

42. Teschner D, Farra R, Yao L, Schlögl R, Soerijanto H, Schomäcker R, Schmidt T, Szentmiklósi L, Amrute AP, Mondelli C (2012) An integrated approach to Deacon chemistry on RuO2-based catalysts. J Catal 285(1):273–284

43. Cheng H, Lin W, Li X, Zhang C, Zhao F (2014) Selective hydrogenation of m-dinitrobenzene to m-nitroaniline over Ru-SnO$_x$/Al$_2$O$_3$ catalyst. Catalysts 4(3):276–288

44. Parnian MJ, Najafabadi AT, Mortazavi Y, Khodadadi AA, Nazzari I (2014) Ru promoted cobalt catalyst on γ-Al_2O_3: Influence of different catalyst preparation method and Ru loadings on Fischer–Tropsch reaction and kinetics. Appl Surf Sci 313:183–195

45. Wang X, Tian JS, Zheng YH, Xu XL, Liu WM, Fang XZ (2014) Tuning Al_2O_3 surface with SnO_2 to prepare improved supports for Pd for CO oxidation. ChemCatChem 6(6):1604–1611

46. Michorczyk P, Kuśtrowski P, Chmielarz L, Ogonowski J (2004) Influence of redox properties on the activity of iron oxide catalysts in dehydrogenation of propane with CO_2. React Kin Catal Lett 82(1):121–130

47. Afandizadeh S, Foumeny E (2001) Design of packed bed reactors: guides to catalyst shape, size, and loading selection. Appl Therm Eng 21(6):669–682